

Kinetic limits for sensing tip morphology in near-field scanning optical microscopes

B. I. Jakobson, P. J. Moyer,^{a)} and M. A. Paesler^{a)}

Department of Physics, North Carolina State University, Raleigh, North Carolina 27695-8202

(Received 31 August 1992; accepted for publication 25 February 1993)

The lateral spatial resolution provided by near-field scanning optical microscopes depends critically on the shape and size of the sharpened tip of the optical fiber used as a source of light or sensing element. The fabrication of a tip by the commonly used heating and pulling method is examined. It consists of an initially pulling and rupture followed by a cooling and relaxation. The presented analysis leads to a deeper physical understanding of these processes and suggests avenues for technical improvements.

A number of optical imaging instruments have been developed^{1,2} that provide lateral spatial resolution much finer than that available in conventional optical microscopes, which are limited by the effects of diffraction. These super-resolution instruments are based on the use of small apertures or sharpened tips as sensing elements. Although there are a number of distinct modes of operation, most involve the passage of an optical signal through a sharpened optical fiber placed very near the structure being imaged. In the following study, we concentrate on one particular type of such instrument, the near-field scanning optical microscope, or NSOM. The analysis of tip morphology and its role in signal transduction and imaging is not a function of the configuration of the imaging instrument, so the analysis might equally apply to other configurations such as the photon scanning tunneling microscope, or PSTM.³ Although the signal transduction mechanism for any of these instruments is a matter of some discussion,⁴ the importance of sensing tip size and morphology in instrument operation is universally accepted. Subwavelength optical resolution clearly depends on the use of a tip with very small radius of curvature.

Given the importance of tip size and morphology, it is reasonable to closely examine current NSOM sensor tip fabrication techniques. These typically involve an adaptation of a heating-and-pulling method developed in the pipette industry, which has accumulated considerable experience and obtained results satisfactory for quite different needs.⁵ In NSOM applications, the crucial optical role of the tip morphology and especially the final radius of curvature makes any decrease of the latter and better control of the former very desirable. These goals can be achieved by more targeted fabrication procedure based on deeper physical insight. The purpose of the present communication is to examine in more detail the physical process that occurs when a fiber is drawn to a fine point during the heating-and-pulling method.

The formation process that determines the final tip shape and sharpness, includes two stages: (i) the pulling and rupture of a fiber heated to some elevated temperature

T_h and (ii) subsequent cooling and relaxation until viscous flow is negligible. The initial radius at the moment of rupture, r_p , can be estimated by considering it as a result of two competing phenomena: (a) a uniform thinning caused by the externally applied tension p ; and (b) an intrinsic capillary instability of the cylinder due to the surface tension γ , which tends to neck off the fiber into separate parts with smaller total surface area. Competition between these effects can be described in terms of their characteristic times.

The elongation of a fiber segment under external stretching force results in its thinning. The instantaneous rate of the radius decrease should be proportional to the pulling pressure p and inversely proportional to the glass viscosity v . Thus,

$$\left(\frac{1}{r}\right) \frac{dr}{dt} = -\frac{p}{v} \quad (1)$$

and a characteristic time of thinning $\tau_t = v/p$ can be introduced. In the absence of other phenomena leading to rupture and tip formation (and neglecting any effects due to gravity or environmental perturbations) one could expect unlimited thinning up to a cylinder of atomic diameter. The cylinder, however, is not a minimal free energy shape for a given quantity of material. This was first demonstrated by Plateau, and the dynamics was elaborated upon by Lord Rayleigh (who referred to as "varicose" instability). In the case we are interested in, when surface tension and viscosity are paramount (rather than gravity and inertia⁶), any surface perturbation with a wavelength greater than $2\pi r$ will grow. There is no finite mode of maximum instability, which means that a fiber (even homogeneously heated) would give way at a few and distant places rather than break up into a sequence of drops. The characteristic time associated with this capillary instability is⁶ $\tau_c = (v/\gamma)r$.

Fiber thinning continues homogeneously until the interference of the instability is negligible, i.e., until its characteristic time τ_t is reasonably shorter than that of capillary necking τ_c . The path representing the actual pulling might follow the curved line in Fig. 1, which depicts characteristic thinning time versus the instantaneous fiber radius, provided that tensile force p is defined for every r for some regime of pulling. The initial tip will be formed when this

^{a)}Also at: Precision Engineering Center, North Carolina State University, Raleigh, NC 27695-8202.

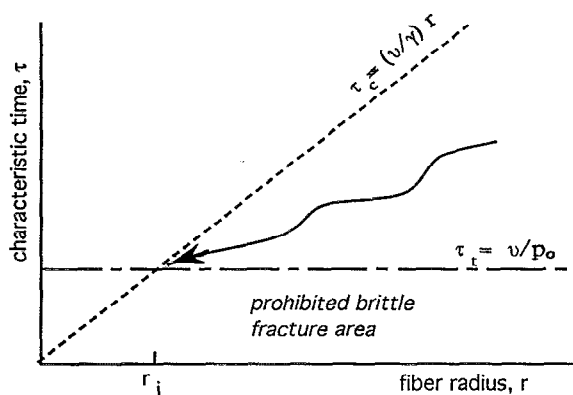


FIG. 1. Characteristic times vs radius for two competing effects in fiber pulling. The pulled fiber necks off when the curved line representing the pulling path intersects the dashed line, which gives the capillary necking time. The time associated with pure thinning (dashed-dotted line) can be made as low as possible on the plot by increasing the external pulling pressure, p , up to the limit of fiber rupture, p_0 .

path intersects the dashed capillary “pinch-off” line (τ_c vs r). An important restriction related with glass rheology should be kept in mind: the tension (or, equivalently, the strain rate) must be lower than certain threshold value p_0 to avoid brittle fracture of the fiber.⁷ This condition holds above the horizontal dashed-dotted line representing $\tau_t = v/p_0$ in Fig. 1. An optimal (i.e., smallest r_i) initial tip is formed when the curved line intersects τ_c at the intersection of the line segments representing τ_c and τ_t . The initial tip radius $r_i \approx \gamma/p$ is generally well above its lower bound γ/p_0 . For a glass surface energy of 1 J/m^2 and strength of 1 GPa one obtains a 1 nm radius limit. Thus, at this first stage an ultimately atomically sharp tip may be possible as soon as low surface energy and maximum fiber strength during the pulling are attained.

In current NSOM tip production, capillary thinning results in the rupture that creates the initial tip of radius r_i . This same process, however, can lead to undesirable results when multiple instabilities occur before one instability has led to fiber rupture. This is illustrated in Fig. 2 where electron micrographs of two pulled tips are shown. The simple conical tip [Fig. 2(a)] represents a structure that could serve as an NSOM tip. It has a small radius of curvature and an adiabatic taper. Its initial radius r_i was apparently formed when only one capillary instability of any consequence occurred during the pulling process. The tip in Fig. 2(b) is an example of what can result when multiple (in this case two) capillary instabilities occur before rupture. Such a tip is neither mechanically nor optically well suited for NSOM use.

After the formation of the initial radius r_i , the substantial Laplace pressure γ/r combined with the low viscosity of the still-hot glass may result in tip blunting. Any precise description of this process would represent an extremely complex fluid dynamic problem of viscous flow. The following approximation retains all important features yet is still tractable. Very roughly, the geometry of the tip can be characterized by one variable which is tip curvature radius $r \gg r_i$ at every moment. The rate of the relative increase of

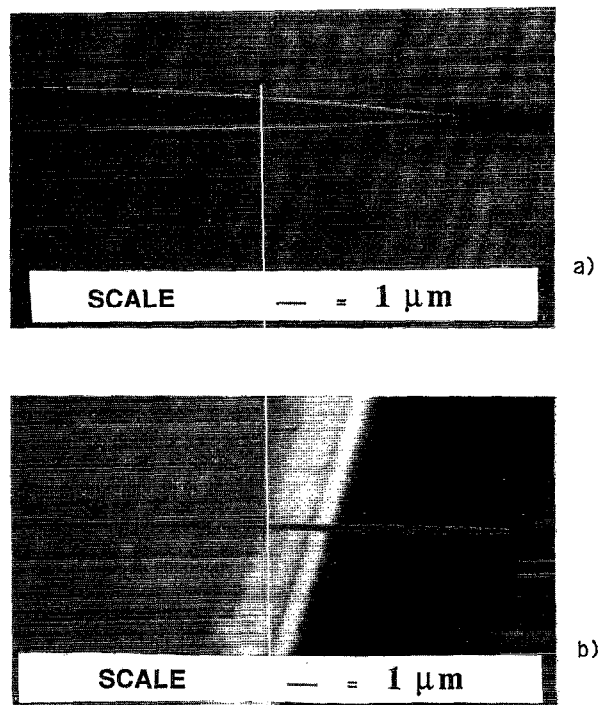


FIG. 2. Electron micrographs of pulled NSOM tips. (a) Represents a shape and size well suited for NSOM use while (b) shows a tip that was formed when two capillary instabilities occurred before fiber rupture. This tip is not well suited for NSOM use.

this radius must be proportional to the “driving force” of the blunting (which is the Laplace pressure) and inversely proportional to the viscosity, $(1/r)dr/dt = (\gamma/r)/v(T)$. So, the simple relation follows:

$$\frac{dr}{dt} = \frac{\gamma}{v(T)} \quad (2)$$

This process practically stops as soon as tip cools down to the glass transition temperature T_g and viscosity increases tremendously. Whatever the details of local fiber heating are (laser beam irradiation in most cases) some region of size larger than r has an elevated temperature T near or above approximately 1000°C . In this situation elementary estimates show that among three channels of the heat dissipation thermal radiation is greater than convective heat transfer to the air and much larger than heat conduction through the glass itself. This means that, with the heater (laser beam) off, the temperature of the tip follows the equation

$$\left(\frac{dT}{dt}\right)cr^3 = \sigma T^4 r^2, \quad (3)$$

where c is specific heat (per unit volume), $\sigma = 5.67 \times 10^{-8} \text{ J/s/m}^2/\text{K}^4$ is the Stefan-Boltzmann constant, and the backward radiation flux from the environment (of temperature $T_0 < T < T_h$) is neglected. Assuming that the heat source is switched off at the very moment of fiber rupture, one can eliminate time from the Eqs. (2) and (3) and obtain after integration,

$$\ln r_f = \ln r_i + \int_{T_0}^{T_h} \frac{c\gamma}{\sigma T^4 v(T)} dT. \quad (4)$$

It is convenient then to adopt an empirical extrapolation for the viscosity,^{7,8} $v(T) \approx V \exp(A/T)$, and to proceed with integration in the second term, representing tip relaxation:

$$\ln r_f = \ln r_i + \left(\frac{\gamma c}{\sigma} \right) \frac{1}{VA^3} \left[\left(\frac{A}{T_h} \right)^2 + 2 \left(\frac{A}{T_h} \right) + 2 \right] \times \exp \left(- \frac{A}{T_h} \right). \quad (5)$$

It is instructive to express the above relation in the form

$$\frac{r_f}{r_i} = \exp \left\{ \left[\left(\frac{\gamma c}{\sigma} \right) \frac{1}{VA^3} \right] \Theta(T_h) \right\}. \quad (6)$$

From Eq. (6) it is clear that the amount of post-rupture relaxation is represented by the product of two terms in the argument of the exponential, one involving material parameters, and the other, $\Theta(T_h)$, incorporating the temperature dependence of thermal relaxation.

To evaluate the contribution of each of these terms to the final tip radius, we first assume that $\gamma \approx 1 \text{ J/m}^2$, $c \approx 2 \times 10^6 \text{ J/m}^3/\text{K}$ (typical value for glasses) and $V = 6.3 \times 10^{-9} \text{ kg/m/s}$, $A = 6.3 \times 10^4 \text{ K}$ for SiO_2 . With these values, the temperature independent factor $(\gamma c/\sigma)(V/A^3) = 10^7$ is quite large. The temperature dependent term, $\Theta(T_h)$ is a strongly varying function of the heating temperature and is in most applications very small. At the working point⁷ ($v \approx 10^3 \text{ kg/m/s}$, $T \approx 2500 \text{ K}$ for SiO_2) the temperature relaxation factor is about $\Theta \approx 10^{-8}$ so that the relaxation contribution to the final tip radius is on the order of a few percent at most, due to relatively high glass transition temperature and “activation energy” for this material an (as a result) fast cooling and solidification. Only if the heating temperature, T_h , were extremely high—on the order of 3000 K—would relaxation play a role in tip radius determination. In most conceivable laboratory situations in tip-pulling settings, such a high temperature would never be achieved. Furthermore, to keep the prefactor of this term small, minimization of the surface tension, γ , is desirable. The latter condition might be realized through introduction of an ambient other than air during the pulling process.

Our analysis suggests that post-rupture relaxation hardly ever comes into play in normal tip manufacture. It does not address, however, the observed shape of drawn tips. Normally the approximation that the shape is spherical at the very tip breaks down under close scrutiny. A flattening of the tip is often observed in the sharpest tips when examined in a high resolution electron microscope.⁹ One can reasonably assume that the bluntness of the very tip is a result of brittle fracture, rather than viscous necking. This would correspond to the situation when the “pulling trajectory” intersects the horizontal line (of brittle fracture threshold) in Fig. 1.

While this analysis appeals to several approximations and simplifications, it does identify the mechanisms involved in NSOM tip fabrication by the heating and pulling method, and it provides recommendations for optimal tip fabrication. In particular, the initial radius of curvature r_i may be minimized by: (i) employing maximum tension below the glass rupture threshold; and (ii) decreasing the surface tension γ . Once rupture is complete and the cooling and relaxation stage has begun, the final radius r_f may be minimized if: (i) the pulling has been undertaken at as low a temperature T_h as can be reasonably experimentally allowed; and (ii) the surface tension is as low as possible. Given the optical and thermal properties of SiO_2 , these results are consistent with the experimental observation that for CO_2 laser tip pullers large pulling forces and high laser power result in small radius tips.

Due to the valuable complementary information available from NSOM and force microscopy, a combined NSOM/shear force microscope has recently been reported.¹⁰ Since in this case the optical fiber serves as a force transducer as well as an optical probe, its mechanical properties are important. Although the analysis above focuses primarily on tip radius, the tip geometry, and radius both determine its transverse rigidity, natural frequencies, and quality factor. Insofar as optical and mechanical performance is important in a combined optical/shear force instrument, and since both will be affected by tip morphology, an extension of the above study to consider both tip radius and shape is clearly indicated.

We gratefully acknowledge helpful conversations with E. Buckland, C. Jahncke, and A. La Rosa as well as with colleagues in the Precision Engineering Center. One of us (BIY) is grateful to G. Ryskin for useful discussion. Work was supported by the Army Research Office (DAAL03-91-G-0053) and the industrial affiliates of the Precision Engineering Center. Among the latter, we particularly thank Digital Instruments for their help.

¹S. Manne, SPIE 1639 (1992).

²E. Betzig and J. Trautman, *Science* **257**, 189 (1992); E. Betzig, J. Trautman, T. D. Harris, J. S. Weiner, and R. L. Kostelak, *Science* **251**, 1468 (1991).

³R. C. Reddick, R. J. Warmack, and T. L. Ferrell, *Phys. Rev. B* **39**, 767 (1989).

⁴E. L. Buckland, P. J. Moyer, and M. A. Paesler, *J. Appl. Phys.* **73**, 1018 (1993).

⁵Many NSOM laboratories adapt commercially available pipette-pullers (such as those available from Sutter Instruments) to serve as optical fiber-pullers to make NSOM sensing elements. See also, K. T. Brown and D. G. Flaming, *Advanced Micropipette Techniques for Cell Physiology* (Wiley, Chichester, 1986).

⁶S. Chandrasekhar, *Hydrodynamic and Hydromagnetic Stability* (Oxford University Press, New York, 1961), Chap. 12.

⁷R. H. Doremus, *Glass Science* (Wiley, New York, 1973), Chaps. 6 and 15.

⁸S. E. Miller and A. G. Chynoweth, Ed., *Optical Fiber Telecommunications* (Academic, San Diego, CA, 1979), Chaps. 7 and 12.

⁹E. Betzig and J. K. Trautman (private communication).

¹⁰E. Betzig, P. L. Finn, and J. S. Weiner, *Appl. Phys. Lett.* **60**, 2484 (1992).